Hydrol. Earth Syst. Sci., 15, 2821–2837, 2011
www.hydrol-earth-syst-sci.net/15/2821/2011/
doi:10.5194/hess-15-2821-2011

Hydrology and Earth System Sciences

Sediment transport modelling in a distributed physically based hydrological catchment model

M. Konz[1], M. Chiari[2], S. Rimkus[1], J. M. Turowski[3], P. Molnar[1], D. Rickenmann[3], and P. Burlando[1]

[1]Institute of Environmental Engineering, ETH Zurich, Wolfgang-Pauli-Str. 15, 8093 Zurich, Switzerland
[2]Institute of Mountain Risk Engineering, University of Natural Resources and Life Sciences, Peter Jordanstr. 82, 1190 Vienna, Austria
[3]Mountain Hydrology and Torrents, Swiss Federal Research Institute, WSL, Zürcherstr. 111, 8903 Birmensdorf, Switzerland

Received: 10 August 2010 – Published in Hydrol. Earth Syst. Sci. Discuss.: 4 October 2010
Revised: 10 August 2011 – Accepted: 26 August 2011 – Published: 9 September 2011

Abstract. Bedload sediment transport and erosion processes in channels are important components of water induced natural hazards in alpine environments. A raster based distributed hydrological model, TOPKAPI, has been further developed to support continuous simulations of river bed erosion and deposition processes. The hydrological model simulates all relevant components of the water cycle and non-linear reservoir methods are applied for water fluxes in the soil, on the ground surface and in the channel. The sediment transport simulations are performed on a sub-grid level, which allows for a better discretization of the channel geometry, whereas water fluxes are calculated on the grid level in order to be CPU efficient. Several transport equations as well as the effects of an armour layer on the transport threshold discharge are considered. Flow resistance due to macro roughness is also considered. The advantage of this approach is the integrated simulation of the entire basin runoff response combined with hillslope-channel coupled erosion and transport simulation. The comparison with the modelling tool SETRAC demonstrates the reliability of the modelling concept. The devised technique is very fast and of comparable accuracy to the more specialised sediment transport model SETRAC.

Correspondence to: M. Konz et al.
(markus.konz@rms.com)

1 Introduction

Bedload transport in rivers is a problem of considerable scientific and public concern. During heavy rain events significant masses of sediment can be mobilized and transported downstream. The consequences of this include reservoir siltation, blocking of channels which can cause flooding, loss of aquatic habitat and river bank instabilities. Especially in mountainous catchments with channel gradients larger than 0.05 and bed sediment containing a high portion of gravel, cobbles and boulders, transport capacities during flood events can reach very high values and the transport limiting factor is often only the sediment availability. The channel geometry varies largely as well as stream flow velocity and roughness (Hassan et al., 2005). Thus, sediment transport dynamics in these channels may substantially differ from those in low-gradient channels. Due to the socio-economic relevance of sediment transport processes for their potential of water induced natural hazards, accurate simulation and forecasting tools are required. A considerable number of bedload transport models have been developed in the recent decades but most of them have not been tested for steep channels in torrents and are not suitable for the joint simulation of basin runoff response and sediment transport. Two strategies can be followed for sediment routing in steep channels. The first approach consists in using a hydraulic simulation model including a sediment transport module, which allows considering variations in bed geometry due to erosion or deposition processes. These models typically include the full Saint Venant equations for one- or two-dimensional flow combined with

Published by Copernicus Publications on behalf of the European Geosciences Union.

a sediment transport equation together with the so-called Exner equation to account for sediment transport and storage effects in the riverbed. Examples are the one dimensional 3ST1D model (Papanicolaou et al., 2004), the 1.5 dimensional FLORIS-2000 model (Reichel et al., 2000) or the semi two-dimensional stream tube SDAR model (Bahadori et al., 2006). Most two-dimensional bedload transport models have been developed for large riverine or estuarine environments. An example of a two-dimensional model applicable for steep slopes is the Flumen model (Beffa, 2005). The SETRAC model (Rickenmann et al., 2006; Chiari et al., 2010b) has specifically been developed for simulations of steep alpine torrents. These very specialized models allow for simulations of sediment transport in a detailed way. The drawback of these models is, however, that important feedback mechanisms as well as the seriality of processes are hard to study due to the separate treatment of the streamflow modelling and the sediment transport. The answer to this limitation can come from integrated models, which account for both basin hydrology and processes driven by hydrological response, like soil slips and sediment transport in channels. Thus, sediment transport accounting hydrological models were developed, which consider sediment transfer processes at the catchment scale, within the framework of a classical rainfall-runoff model. Examples are the ETC rainfall-runoff-erosion model (Mathys et al., 2003), the SHESED model (Wicks and Bathurst, 1996), the DHSVM model (Doten et al., 2006) or the PROMAB- GIS model (Rinderer et al., 2009).

The rather limited complexity of some of these models is, however, not always adequate to simulate the continuous process of erosion and sediment transport in mountainous catchments. Some other models were conceived for applications in basins characterised by gentle topography and do not include equations specifically suitable for steep channels, which are typical of mountain basins.

Accordingly, this paper focuses on the simulation of sediment transport in steep torrents of alpine catchments. Models for simulations of mountainous catchments require specific modules for simulation of hydrological processes such as snow and glacier melt and routing, while a detailed description of the highly variable channel geometry is needed for the sediment transport simulations. In fact, geometrical properties like channel bed slope and channel width are important variables, which control hydraulics and consequently bedload transport. Usually, a high resolution grid is a prerequisite for the detailed description of channel geometry. However, model simulations demand more CPU with increasing resolution and basin wide simulations become inefficient and slow. In this paper we added a module for the simulation of the temporal evolution of river bed sediment dynamics at the catchment scale to the distributed physically-based hydrological model TOPKAPI. The innovative aspect of the newly introduced sediment module is the sub-grid simulation of the sediment routing, which takes advantage of the more detailed description of the channel geometry at the sub-grid level, and the efficient hydrological and hydraulic simulations on the coarser grid level used for the simulation of the catchment hydrology. The aim of this paper is to describe the implementation of the sub-grid sediment modelling scheme and to present the evaluation of the newly developed sediment module against the more specialized SETRAC model as a model inter-comparison. In order to corroborate the findings from the intercomparison, we use, rather than a hypothetical case study, the 2005 flood event in the Bernese Alps, Switzerland. Although the available data base of this event has been reconstructed from post-event observations and is thus affected by some limitations in terms of error quantification, it provides a case to test the model in a realistic basin and channel morphology and topography context. As such, it allowed, as further discussed in the subsequent sections, to highlight the relevance of using a reduced energy slope due to macro-roughness flow resistance. It must be therefore clear to the reader that the aim of this work is not to reproduce the sediment balance of the storm event in detail, being this a difficult task due to the hardly quantifiable observational error: it is rather a comparison of a model specialized in channel sediment transport with a more agile and, above all, catchment scale hydrological model capable of matching the performance of the specialized model.

2 Study site and extreme event in August 2005

Many regions in Austria, Switzerland and Germany were affected by the flood events in August 2005 (MeteoSchweiz, 2006). A massive cyclone over the northern part of Italy caused heavy rainfall particularly from 21–22 August 2005. The period of relevant precipitation was about four days, whereas thunderstorms were not of major importance. In Switzerland the whole north-alpine region was affected by heavy rainfall that triggered widespread flooding. The highest precipitation sums for a 72-h period were measured in Switzerland, where more than 250 mm were observed across the Alps, with the highest sums observed in Gadmen, 320 mm, Rotschalp, 283 mm, Weesen, 277 mm, and Amden, 267 mm (MeteoSchweiz, 2006).

For testing of the newly developed sediment transport routine in TOPKAPI we selected the Chiene catchment in the Bernese Alps that was heavily affected by the storm event. The catchment is situated in the Canton Berne, the catchment area is 90.5 km^2, and it is drained by the main river Chiene and the tributary Spigge (see Fig. 1). As discussed by Chiari and Rickenmann (2011) no streamflow measurements for the Chiene mountain river are available, but the discharge was reconstructed with streamflow measurements located (see Fig. 1) on the river Kander 6 km upstream (in Frutigen) and 6 km downstream (in Hondrich) of the confluence with the Chiene (Rickenmann and Koschni, 2010).

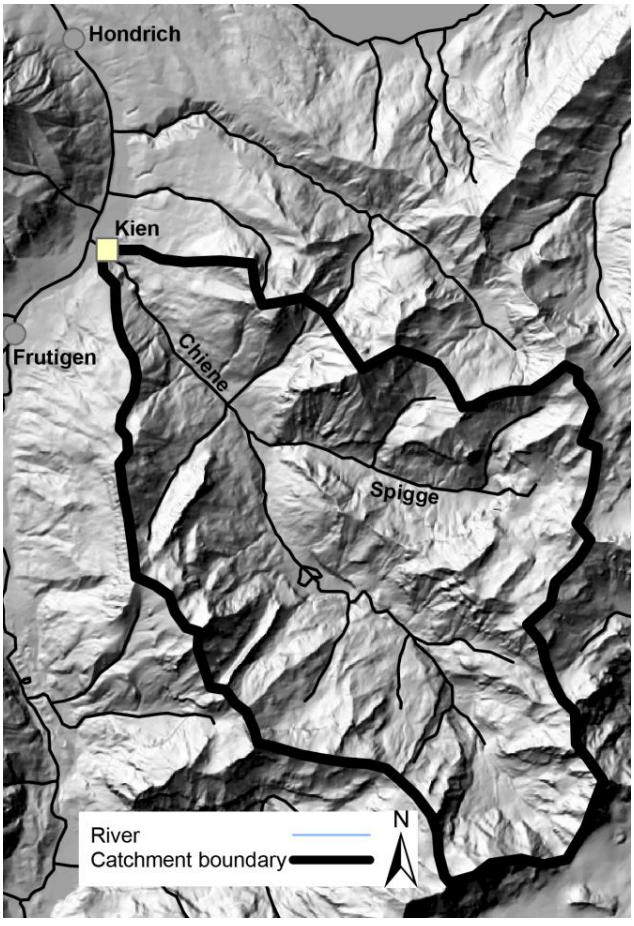

Fig. 1. Chiene catchment area and location of gauging stations for discharge reconstruction.

The Chiene is a steep mountain stream with a mean channel gradient of 0.05. The slope is ranging from 0.004 in the flat middle reaches up to 0.17 in the steepest reaches (Fig. 2c). The channel width has a maximum of around 150 m between 5.5 and 6.2 km. The initial sediment storage depth was estimated in the field between 1 and 5 m. This estimate refers to a possible volume of sediment which may have been entrained during the flood from the bed and the banks, and this volume is divided by the channel width and the unit stream length of 1 m. This assessment was made for all channel reaches, and the estimated value depends for example on the presence of large boulders inhibiting or slowing down erosion or of bedrock limiting the maximum erosion depth. The grain size distributions were estimated with a transect-by-number analysis and evaluated after Fehr (1986), values were taken from Chiari et al. (2010b). Two LiDAR based digital elevation models (DEM) are available for the catchment, representing the pre- and post-flood situation. Morphologic changes in torrents and mountain rivers are only caused by major flood events. No other flood events have been reported for the time span between the two LiDAR flights. Chiari et al. (2010b) derived the transport volumes from these LiDAR based DEMs.The volumetric analysis was carried out using the methodology illustrated by Scheidl et al. (2008) and compared qualitatively with aerial photographs and completed with data from sediment redistribution during the flood recovery phase (LLE Reichenbach, 2006). During the event, about 120 000 m^3 of bedload were mobilized. Most of the material was deposited in the flat middle reaches (5.3 km to 6 km) and in the village of Kien, close to the confluence with Kander river. The LiDAR analysis indicated that there was more deposition in the flat middle reaches (5.5 km) than sediment input from upstream areas not covered by the LiDAR flight. Therefore, we considered at 8.3 km (see Fig. 2a) a sediment input of about 20 000 m^3 from that area, which can be assumed, if we consider an error estimate comparable to that found by Scheidl et al. (2008) to be in agreement with field observations (LLE Reichenbach, 2006). This allowed assessing the sediment supply over the entire catchment area. We refrain here from a detailed discussion about error estimates of the reconstructed sediment supply, since we use these data only as qualitative reference for the comparison between the two models. An error of $\pm 25\,\%$ of the reconstructed sediment transport rates as suggested by Scheidl at al. (2008) is shown in Fig. 2a as grey band around the estimated value.

3 The TOPKAPI model

TOPKAPI has originally been developed at the University of Bologna (Italy) as a physically based distributed hydrological catchment model (Todini and Ciarapica, 2001; Liu and Todini, 2002; Liu et al., 2005). The model simulates all relevant components of the water balance and models the rainfall-runoff (R-R) processes by means of non-linear reservoir equations, which represent drainage of the soils, overland flow and channel flow and are obtained by the integration of the topographic kinematic approximation of the flow equations (Todini and Ciarapica, 2001). The relevant information about river network topology, surface roughness and soil characteristics are obtainable from digital elevation models, soil and land use maps.

The Hydrology and Water Resources Management Chair of ETH Zurich, Switzerland, has further developed TOPKAPI to make it applicable to high alpine regions. Among other things a new snow and ice melt routine has been implemented that enables the distributed simulation of snow accumulation and melt as well as glacier melt. Moreover, modules to simulate water induced geomorphological processes like soil slips, hillslope erosion and channel sediment transport have been implemented to mimic storm rainfall driven processes. In the following a brief overview of the R-R transformation components will be given, whereas the channel sediment transport module will be described in detail.

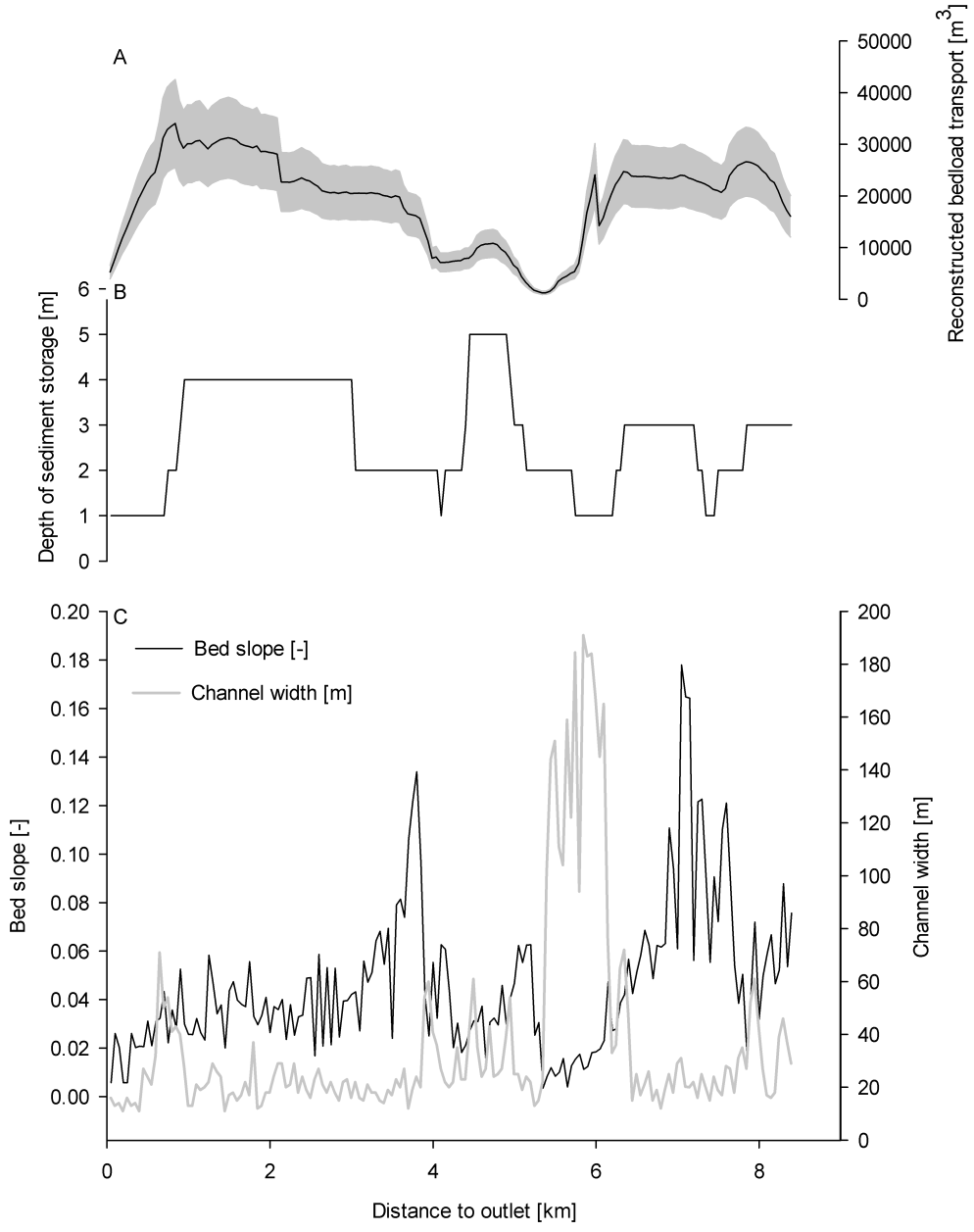

Fig. 2. Properties of the Chiene river and observations of bedload transport. **A**: Reconstructed bedload transport, the grey band indicates a ±25 % error band, **B**: initial depth of sediment storage, **C**: bed slope of the river and channel width.

3.1 The R-R model components in TOPKAPI

The R-R model components can by grouped into four major modules: (i) the module to generate spatially distributed meteorological input variables, (ii) the snow and glacier module, (iii) the soil and runoff generation module, and (iv) the channel routing module. The R-R response is simulated in a distributed grid-based approach and within one time step the model simulates the water cycle components for each grid cell accounting for topographic constraints. Meteorological input variables (temperature and precipitation) can be provided as maps or as point measurements. Appropriate elevation dependent lapse rates are used in the interpolation routine to generate spatial temperature and precipitation fields if point measurements are provided. Snow and ice melt is simulated applying the Enhanced Temperature Index (ETI) model (Pellicciotti et al., 2005) with a computed potential clear-sky global irradiance as described by Corripio (2003). Water from snow melt and rain infiltrates into the soil unless the soil is already saturated. Together with inflowing water from upstream and lateral cells, this vertical infiltration

yields the soil water content. Overland flow occurs if the maximum soil water storage is exceeded. This is equivalent to a saturation excess runoff generation mechanism. Actual evapotranspiration is calculated as a function of the soil water content and potential evapotranspiration if the water content is below a certain threshold. Otherwise, actual evapotranspiration equals the potential evapotranspiration, which is computed with the Makkink approach (Deyhle et al., 1996).

Water fluxes in the soil are obtained by combining the dynamic equation (Eq. 1) with the equation for continuity of mass (Eq. 2).

$$q = \tan(\beta) k_s L \Theta^b \tag{1}$$

$$p = (\vartheta_s - \vartheta_r) L \frac{\partial \Theta}{\partial t} + \frac{\partial q}{\partial x} \tag{2}$$

Here q is the horizontal flow in the soil in $m^2\,s^{-1}$, p is the intensity of vertical inflow in $m\,s^{-1}$, t is time in s, x is the direction of flow along a cell in m, β is the slope angle as radiance, b is an empirical parameter which depends on the soil characteristics, k_s is the saturated hydraulic conductivity in $m\,s^{-1}$, L is the thickness of the soil layer in m, Θ is the mean value along the vertical profile of the soil water content, ϑ_s is the saturated soil water content and ϑ_r is the residual soil water content.

Two soil layers can be used to simulate interflow and base flow components. Overland flow is computed with a comparable approach but Manning's formula is used in place of the dynamic equation. Soil erosion on hillslopes is computed based on simulated overland flow. The hillslopes are coupled to the river channel and the mobilised mass fills the sediment storage of the river if the sediment reaches the river. The hillslope erosion module is, however, not discussed here and has not been used in this study, because the focus of this paper is set on channel sediment transport simulations during flood events and the benchmark model SETRAC does not simulate hillslope erosion. An additional module, which has been added to the model but is not described here, allows the simulation of slope failures by computing the factor of safety on the basis of the soil water dynamics, thus allowing to compute localized sediment supply. Finally, flow routing in the channel is particularly important for sediment transport simulations and is therefore described in detail in the next section.

3.2 Channel flow routing

Channel flow is described with a kinematic wave approximation similar to overland flow, thus describing the flow dynamics by means of Manning's formula (Eq. 3) and of the continuity equation shown in Eq. (4), that is

$$q_c = \frac{1}{n_c} \sqrt{S} \left(\frac{B}{C} \right)^{2/3} B y_c^{5/3} \tag{3}$$

$$\frac{\partial V_c}{\partial t} = \left(r_c + Q_c^u \right) - q_c \tag{4}$$

where q_c is the horizontal flow in the channel in $m^3\,s^{-1}$, n_c Manning's friction coefficient for channel roughness in $m^{-1/3}\,s$, S is the bed slope, B is the channel width in m, C is the wetted perimeter, y_c is the water depth in the channel in m, V_c is the water volume in the channel in m^3, t is time in s, r_c is the lateral drainage input in $m^3\,s^{-1}$, and Q_c^u is the inflow discharge from the channel reach of the upper cells in $m^3\,s^{-1}$. The channels are assumed to be rectangular.

The three non-linear reservoir equations representing soil flow, overland flow and channel flow can be solved analytically as discussed in detail by Todini and Mazzetti (2008). This enables a very efficient computation of the flow processes.

Discharge is simulated in each grid cell that is assigned to as a channel cell. In TOPKAPI the cell length is automatically the length of the river section in this cell, whereas the channel width can be defined as a fraction of the cell size. The bed slope is derived from the DEM.

Flow resistance due to grain roughness plays a crucial role in steep headwater streams and is considered in TOPKAPI by a variable Manning friction coefficient. The Manning coefficient conventionally used by TOPKAPI has been modified to account for dependence on flow depth, and is therefore expressed as a function of discharge, bed slope and the characteristic grain size of the channel bed material that is

$$\text{for } S \geq 0.008 \tag{5}$$

and

$$n_c = \frac{S^{0.03} d_{90}^{0.23}}{4.36 g^{0.49} q_c^{0.02}} \text{ for } S \leq 0.008 \tag{6}$$

where g is the gravity acceleration and d_{90} is the grain size of the bed material for which 90 % of the bed material is finer by weight. These equations were derived from more than 300 field measurements in torrents and gravel bed rivers (Rickenmann, 1994, 1996).

3.3 Sediment transport in TOPKAPI

3.3.1 The sub-grid modelling scheme

TOPKAPI uses square raster cells for spatial discretization and the rivers are represented as predefined sections of the raster cells (Fig. 3a). For sediment transport simulations this discretization of the channel is generally too coarse. Therefore, sub-grid cross-sections of different length and width can be used within each grid cell and different properties can be assigned to these cross-sections (Fig. 3b). The properties are width, length, initial sediment storage depth, slope and grain size distribution. Discharge is simulated at the grid cell level (Fig. 3a) and is assumed to be constant for all sub-grid cross-sections (stationary conditions within a time step,

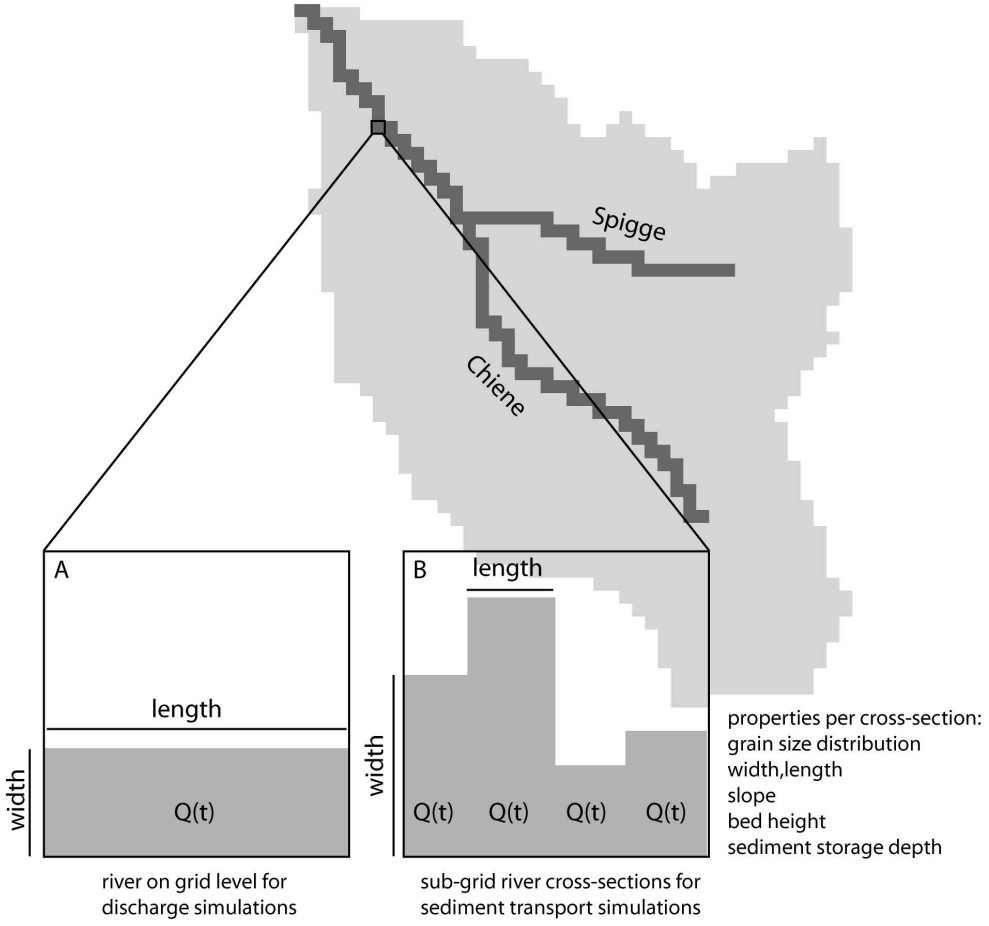

Fig. 3. Sub-grid concept of river cross-sections. **A**: River representation for hydraulic simulations on the grid level; **B**: Sub-grid cross-sections for sediment transport simulations.

Fig. 3b). There is no feedback mechanism between sediment transport simulations and hydraulic simulations, which means that for the hydraulic simulations the channel geometry is constant through time.

In order to avoid rapid exhaustion of the sediment storages the time step length can be decreased to a fraction of the global time step used for the hydrological simulations. The choice of the sub-grid time step is further discussed in Sect. 6. The sediment transport simulations described in the following sections are conducted on the sub-grid level.

3.3.2 Sediment transport capacity

For the calculation of the sediment transport capacity various bedload transport formulas and adjustment methods can be selected in order to adapt the model to the catchment conditions. In the following we provide the equations used to simulate the storm event in August 2005 in the Chiene catchment, Bernese Alps (see Sect. 1 for the description of the event).

Only a limited number of bedload formulas have been developed for steep gravel streams mainly in laboratory flumes. The following formula (Rickenmann 1991, 2001) has been selected to estimate the transport capacity (q_{pot} in m^2 sediment s^{-1}):

$$q_{\text{pot}} = 3.1\left(\frac{d_{90}}{d_{30}}\right)^{0.2}\left(q_{\text{c,s}}(t) - q_{\text{crit}}\right)S^{1.5}(s-1)^{-1.5} \quad (7)$$

where d_{30} is the characteristic grain size for which 30 % by weight is finer, $q_{\text{c,s}}(t)$ is the specific discharge in $\text{m}^2\,\text{s}^{-1}$, q_{crit} is the specific critical discharge $\text{m}^2\,\text{s}^{-1}$and s the ratio between sediment and fluid density ($s = \rho_{\text{s}}/\rho_f$). According to evaluations of several bedload transport formulas, a mathematically almost identical version of Eq. (7) (Rickenmann, 2001) is among the better performing approaches when compared to a large number of flume data (Recking et al., 2008) or extensive field data (Khorram and Ergil, 2010) , and it was also applied to further bedload transport observations in steep and rough streams with some success (Nitsche et al., 2011).

Sediment transport starts once the critical discharge is exceeded. A number of formulations exist to estimate the

critical discharge. Among the five different formulae that have been implemented in TOPKAPI the following relationships according to Rickenmann (1990), have been chosen for the simulations:

$$q_{\text{crit}} = 0.065(s-1)^{1.67} g^{0.5} d_{50}^{1.5} S^{-1.12} \tag{8}$$

$$q_{\text{crit}} = 0.143(s-1)^{1.67} g^{0.5} d_{65}^{1.5} S^{-1.167} \tag{9}$$

Equations 8 and 9 are based on flume experiments representing mountain rivers (Bathurst et al., 1981). Therefore, it can be assumed that the particle size distribution is representative for field applications of the model. For steep mountain streams with irregular bed topography and low relative flow depth additional flow resistance due to macro-roughness elements at the bed becomes important. However, the above described sediment transport formulae are generally based on flume experiments with rather uniform bed material where the movable bed had a more or less planar surface without bed form structures. Thus, essentially skin drag was present in these experiments. In steep and rough streams the total flow resistance is considerably increased. This could be a reason why the bedload transport formulae often overestimate observed bedload transport, if they are applied to steep and rough channels. Energy losses due to increased roughness (intermediate- and large-scale roughness sensu, Bathurst et al., 1981) have been optionally considered in the model by introducing a reduced energy slope, S_{red} (Rickenmann et al., 2006; Chiari et al., 2010b). In the following the associated increase in flow resistance is referred to as "macro roughness" energy losses. For a given channel reach, S_{red} can be calculated with a flow resistance partitioning approach, depending either on unit discharge or on relative flow depth:

$$\frac{n_{\text{o}}}{n_{\text{c}}} = \frac{0.0756 q_{\text{c}}^{0.11}}{g^{0.06} d_{90}^{0.28} S^{0.33}} \tag{10}$$

$$\frac{n_{\text{o}}}{n_{\text{c}}} = 0.092 S^{-0.35} \left(\frac{y_{\text{c}}}{d_{90}} \right)^{0.33} \tag{11}$$

$$S_{\text{red}} = S \left(\frac{n_{\text{o}}}{n_{\text{c}}} \right)^{\alpha} \tag{12}$$

with a roughness coefficient n_{o} associated with a base-level flow resistance only, and n_{c}. corresponding to the total flow resistance (thus including macro roughness resistance).

According to the Manning-Strickler equation an appropriate value of the exponent a in Eq. (12) should be $a = 2$. Meyer-Peter and Mueller (1948) showed theoretically that the exponent α may vary between 1.33 and 2.0, and from their experiments they empirically determined a value of 1.5. To adapt the reduction of the energy slope to observations of bedload transport, the exponent in Eq. (12) can be varied between the values 1 and 2 (Rickenmann et al., 2006). Therefore a can be used as a calibration parameter within the specified range. Back-estimation of a from bedload data for the Austrian and Swiss flood events in 2005 resulted in a best fit exponent a in the range of about 1.2 to 1.5 (Chiari and Rickenmann, 2011).

Moreover, mountain streams can develop an armour layer if finer sediment fractions are more likely to be transported than coarser fractions. If armouring cannot be neglected this effect can be considered optionally in combination with the modified critical discharge $q_{\text{crit},a}$ (Badoux and Rickenmann, 2008):

$$q_{\text{crit},a} = q_{\text{crit}} \left(\frac{d_{90}}{d_{\text{m}}} \right)^{10/9} \tag{13}$$

with d_{m} as the mean grain size. As shown by this equation the specific critical discharge, q_{crit}, is increased and thus the incipient motion is delayed, which causes reduced sediment transport rates.

The sediment transport capacity is thus finally the maximum amount of sediment that can be transported by the water discharge considering losses due to macro roughness in steep streams and/or effects of armour layers.

The actual sediment transport is subject to sediment availability in the stream channel, defined in the model as sediment storage. The sediment budget per sub-grid cross-section is calculated based on the discrete balancing of incoming sediment, sediment transport capacity and available sediment in the storage using the following equation:

$$\frac{\partial h}{\partial t} = -\frac{\partial q_{\text{s}}}{\partial l} \tag{14}$$

where q_{s} is the specific transported sediment volume in $\text{m}^2\,\text{s}^{-1}$, h is the sediment depth in m and l is the length of the current cross-section in m.

Therefore, both erosion and deposition can be simulated. If the calculated transport capacity exceeds the sediment input from the upstream section, erosion occurs as long as sediment is available in the storage. Erosion is limited by the predefined depth of the sediment layer. The initial sediment volume is defined by the depth of the sediment storage, which is a model input in each sub-grid cross-section. The actually transported sediment is directed to the next downstream cross-section. If the sediment input into the section is larger than the transport capacity, deposition occurs and the sediment storage is filled. During deposition it is possible that the river section becomes blocked and the discharge cannot flow through the section any more. This can especially occur at points with significant changes of the channel slope. If this problem occurs the additional volume that blocks the section is added to the next downstream cell (Fig. 4) and the slope is set to a predefined value of 0.1 %.

After each time step the slope of each cross-section is recalculated according to the following formula in order to simulate a mobile river bed:

$$S = \frac{h_{\text{up}} - h_{\text{dn}}}{l_{\text{dn}}/2 + l_{\text{up}}/2 + l} \tag{15}$$

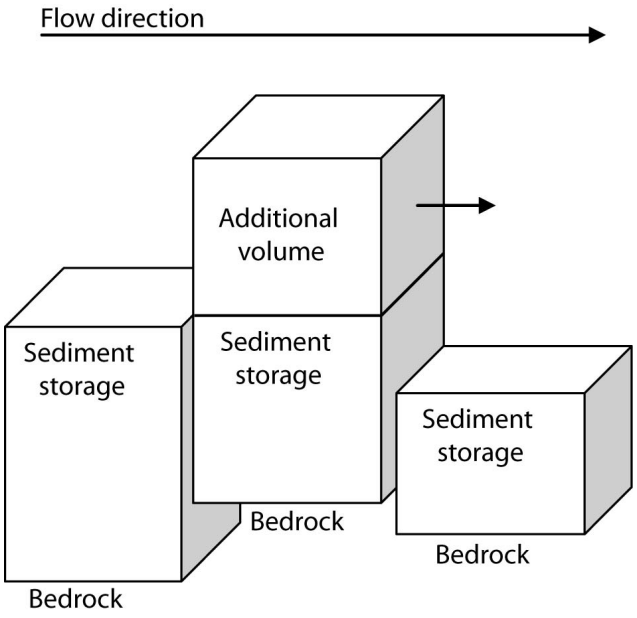

Fig. 4. Redistribution of additional sediment volumes in order to avoid upward slopes.

where h_{dn}, h_{up} are the downstream and upstream river bed heights in m and $l_{dn,up}$ are the downstream and upstream cross-section lengths in m. The newly defined slope is then used for transport simulations in the next time step.

4 The SETRAC model

In this study TOPKAPI is compared to the more sophisticated specialised sediment transport model, Sediment TRansport in Alpine Catchments (SETRAC). SETRAC is briefly described here, focusing especially on the differences between the two models. SETRAC is a one-dimensional model for the simulation of sediment transport in torrents and mountain rivers and was developed at the University of Natural Resources and Applied Life Sciences, Vienna (BOKU), Austria (Rickenmann et al., 2006; Chiari et al., 2010b). The model has been thoroughly tested against laboratory flume data and well documented field events by Chiari (2008) and Chiari and Rickenmann (2011). The channel network is represented by nodes, cross-sections and sections. Nodes contain the information about the location of the related cross-sections. Cross-sections are described by pairs of points containing information about the distance from the left bank and the altitude. Each slice of the cross-section can be of the type main channel, bank or riparian. This discretization allows a detailed description of the cross-section geometry.

Erosion and deposition, as well as bedload transport can only occur in slices of the type main channel. Each cross-section contains information about the grain size distribution, the sediment storage depth and the initial slope. Input hydrographs, simulated in HEC-HMS, can be assigned to cross-sections as time series. Sediment input as time series is also possible. For calculations, the cross-sections are connected by strips to get a representative discretization of the channel. The number of strips depends on the number of slices that are used to specify a cross-section, implying that the number of strips increases with the complexity of the cross-section. Discharge and bedload transport is calculated separately for each strip of the cross-section. The input hydrographs are routed using the kinematic wave approach that is solved numerically by an explicit finite difference method with an upwind scheme. The same sediment transport equations as discussed in the previous section can be used in SETRAC, however SETRAC additionally allows for a fractional bedload transport. Feedback mechanisms of the changing river bed geometry on hydraulic simulations are possible, which is not the case in TOPKAPI. The interested reader is referred to Chiari (2008) and Chiari et al. (2010b) for more detailed descriptions of SETRAC.

5 Simulation of the 2005 event with TOPKAPI and SETRAC

The 2005 flood event in the Bernese Alps was taken as a case study to assess how the sediment transport module implemented in TOPKAPI compares to a dedicated and more sophisticated model like SETRAC. This chapter describes the case specific settings of the models used for the simulations and presents the simulation results of both models. For the simulations, the Chiene as well as its most important tributary Spigge have been considered. In total, 9.77 channel km have been simulated (8.24 km Chiene and 1.44 km Spigge). TOPKAPI has been forced with point information of the meteorological input data temperature and precipitation taken from a meteorological station in Adelboden around 16 km in the South-West of the catchment, which were redistributed by means of appropriate lapse rates. The event duration of 60 h has been simulated using the geometrical information of Fig. 2c, the initial storage depths of Fig. 2b and the grain size distribution provided by Chiari et al. (2010b). 3600 sub-time steps have been taken for the temporal discretization of the sediment routing, which corresponds to a time step length of 1 s compared to 1 h for the hydrological simulations. An equal spacing between the sub-grids of 50 m has been assumed. The grid cell size is $250 \times 250\,m^2$.

Because the major goal of this study is to compare the two models, no particular attention has been paid to the calibration of TOPKAPI hydrologic response. This has been carried out in order to match the reconstructed discharge of the 2005 event (LLE Reichenbach, 2006), which is used as reference value for both models. As already noted in the above sections, an estimate of the error of the reconstructed discharge is not particularly meaningful, as observations are missing and the reconstruction is based on simulations carried out by

a lumped rainfall-runoff model (Rickenmann and Koschni, 2010). However, we assume that the reconstructed and published values, provide at least an order of magnitude of discharge during the event which allows to assess the right order of magnitude of the simulated runoff. Simulations have been done for the entire year 2005 and initial conditions for the sediment simulations of the 60 h event have been taken from these simulations.

The same cross-sections as in SETRAC have been used for TOPKAPI and assigned to the corresponding raster cells. At the confluence point of Spigge and Chiene, one raster cell covers cross-sections of both rivers. It must be noted that the real confluence point is located further downstream with respect to the location identified in the model raster, which, due to the spatial resolution of the grid, locates the confluence point is slightly upstream. Thus, the simulated discharge of this raster cell represents already the merged rivers and is therefore much higher than the discharge of the Spigge cross-sections. In order to avoid overestimations of sediment transport capacities, the cross-sections of Spigge have been shifted upstream by one cell and the sediment output of the last Spigge cross-section is added to the correct cross-section of the Chiene. This modification allows for a more realistic simulation of the hydraulic conditions in the sub-grid cross-section.

The simulated hydrographs used as input to the SETRAC model have been also obtained by matching it to the reconstructed discharge in the different subcatchments. Thus, the 2005 event discharge simulations of both models compare very well, being this a prerequisite for the comparison of the sediment transport simulations. The 50 m spaced cross-sections used for the spatial discretisation every 50 m have been derived from the digital elevation model, which has been generated by airborne LiDAR before the extreme event occurred. It is worth noting that the sediment routine has no calibration parameter if it is used in the full transport capacity mode and only the exponent α can be changed to consider the effect of macro roughness. This parameter is global and cannot be optimised locally, e.g. at the sub-grid cross-section level. Stream channel parameters like width, slope, initial sediment storage are input data as well as sediment input from upstream and from major tributaries, and many of these parameters have to be derived or estimated from field observations.

The sediment transport simulations have been conducted in three different setups, M1 to M3, which differ by the selection of macro roughness equations (Table 1). The simulation results are presented in this chapter as a comparison of SETRAC and TOPKAPI. We also show reconstructed estimates of sediment transport volumes in order to demonstrate the credibility of the simulations. By the application to real data, though affected by errors and uncertainties difficult to quantify in the present case, we intend to show the ability of the scheme adopted in TOPKAPI to mimic a state of the art model for channel erosion and sediment transport, rather than proving the ability of the model to reproduce the overall sediment balance during a storm event.

Table 1. Model setups of TOPKAPI and SETRAC used to simulate the 2005 event. M3 was only used for TOPKAPI.

Model setup	Bedload transport	Incipient motion	Macro roughness effect	Exponent α
M1	Eq. (7)	Eq. (8)	–	–
M2	Eq. (7)	Eq. (8)	Eq. (11)	1.5
M3	Eq. (7)	Eq. (8)	Eq. (10)	1.5

This is well illiustrated in Fig. 5, which shows a comparison of SETRAC and TOPKAPI simulations with the accumulated bedload transport recalculated from the morphological changes. The time integrated bedload transport volumes are shown for the main channel (Chiene). The simulations of TOPKAPI and SETRAC with full transport capacity without any losses due to macro roughness or armour layers (model setup M1) deliver comparable results but overestimate the reconstructed bedload transport. TOPKAPI produces slightly lower bedload transport than SETRAC especially in the downstream part of the Chiene between 0.8 and 2 km. The contribution of the Spigge can be noticed at 6 km in the SETRAC simulations, whereas TOPKAPI only shows a minor reaction to these sediment inputs. In the upper parts of the Chiene both models deliver almost identical results. TOPKAPI simulations with higher critical discharges (not shown here), e.g. by using Eq. (9) instead of (8), are closer to the observed bedload transport, but in several sections no transport is simulated due to a too high incipient motion criteria. Considering an armour layer (Eq. 13) still lead to overestimations of the observations by both models and compared to M1 there is only a small reduction of the total amount of bedload transported during the event (not shown here). It becomes obvious that energy losses due to macro roughness are not negligible. These are considered in model setups M2 and M3 by means of two different equations but α always equal to 1.5 (Fig. 5). Considering energy losses due to macro roughness delivers simulations closer to the observations. TOPKAPI produces higher bedload transport than SETRAC if M2 is taken. M3 in TOPKAPI simulates discharge modified by Eq. (10) which is better suited for correction of high flow resistance with rectangular cross-sections because the water level as used in Eq. (11) depends more on the bed structure than the discharge. Equation (10) is not implemented in SETRAC.

6 Comparison of SETRAC and TOPKAPI

For a detailed comparison of SETRAC and TOPKAPI we analysed the results of setup M1 without losses due to macro roughness but with a variable bed (Fig. 6). SETRAC required

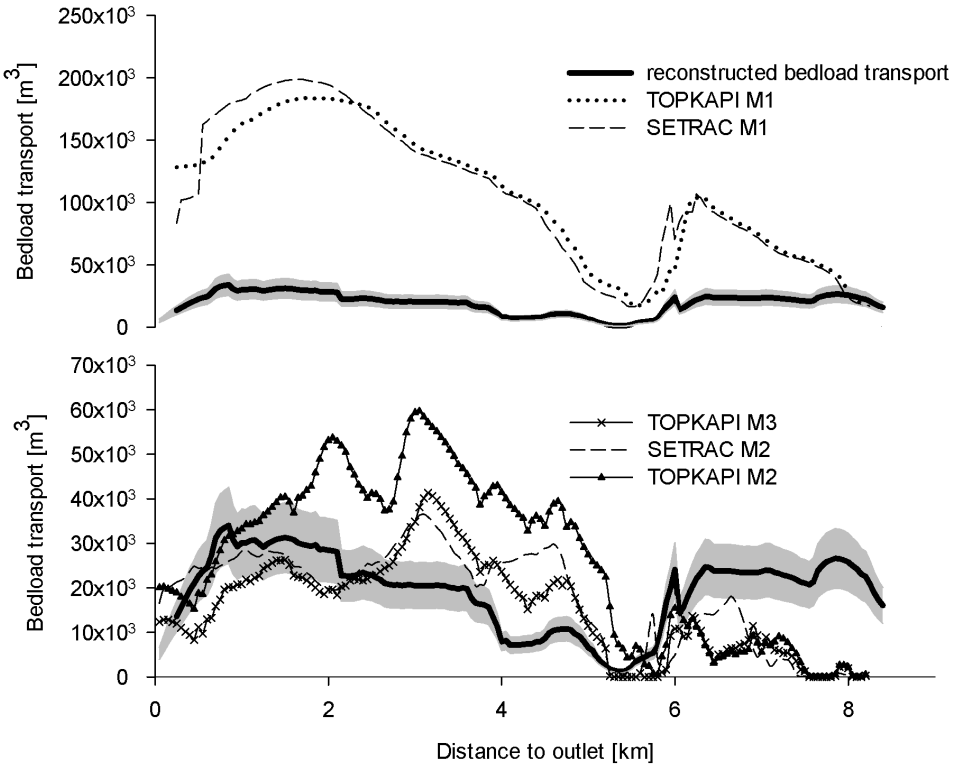

Fig. 5. Comparison of TOPKAPI, SETRAC and reconstructed bedload transport. The grey band indicates the ±25 % error band. Simulations were done with different setups described in Table 1. **A**: Simulations with full transport capacity (M1), **B**: simulations considering losses due to macro roughness using setups M2 and M3. Note that Eq. (10) is not implemented in SETRAC and therefore M3 is only used for TOPKAPI simulations.

around 9 h for the simulations, whereas TOPKAPI needed 40 s. In SETRAC the strip-wise solution of the flow routing and bedload transport requires several iterations. The time step in SETRAC cannot be chosen by the user because the maximum allowed time step is calculated automatically to meet the Courant–Friedrichs–Lewy (CFL) stability criteria and is therefore not constant over the simulation time. During high discharges the time step becomes very small (1.5 s for the presented case study). The time step for sediment routing in TOPKAPI is also small (1 s) but it is only applied on the sediment routing scheme and not on the hydraulic simulations. These are performed on the grid level with an hourly time step.

Figure 6 shows the transport capacities at 10, 30 and 60 h, the accumulated bedload transport, the channel reach slopes and the depth of the sediment storage at the respective time step. The transport capacities produced by TOPKAPI show less fluctuations than the ones by SETRAC. TOPKAPI generally provides smaller transport capacities especially for the peaks at 3.5 and 7.0 km after 30 h. The variable slopes are comparable between the two models, however especially at the last time step SETRAC exhibits pronounced fluctuations of the simulated slopes, whereas TOPKAPI delivers smoothed slopes along the channel. The sediment storage depths of TOPKAPI and SETRAC at 10 and 30 h correspond well. In the last time step, the sediment depths simulated by TOPKAPI are more fluctuating between 1 and 2.5 km compared to SETRAC, and TOPKAPI also simulates an empty storage in the central part and upper reaches of the Chiene. SETRAC delivers fluctuating values between 0 and 1 m for these regions. A systematic difference between the two model outputs can be observed at the confluence of the Spigge and the Chiene at 6.0 km. Although, the bedload transport simulations downstream and upstream of the confluence point are almost identical between the two models, the cross-sections that are directly affected by the confluence show significant differences. SETRAC delivers a much higher bedload transport and the sediment input from the tributary Spigge is clearly visible (peak at 6 km). TOPKAPI only shows a very moderate reaction to the additional sediment input.

7 Discussion

We consider the reconstructed bedload as plausible estimate of the order of magnitude of the real transport rates. In this respect it can be noted that the accuracy of the LiDAR

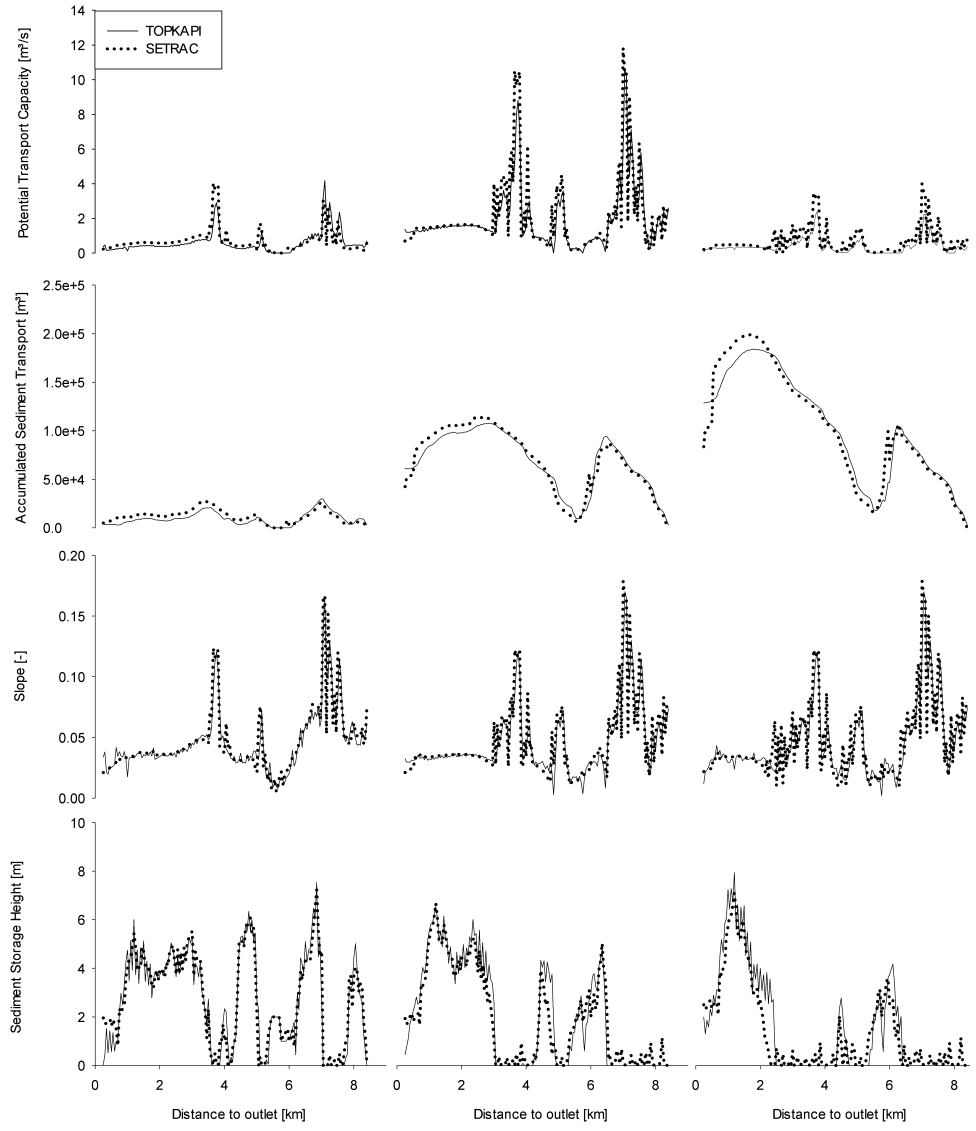

Fig. 6. Detailed comparison of TOPKAPI and SETRAC for setup M1.

analyses is slope dependent (Scheidl et al., 2008) and in particular more accurate for milder reaches. The mean volume error can be determined by 0.3 $m^3\,m^{-2}$ for the analysed catchment (Chiari et al., 2010a).

As expected, both models significantly overestimate sediment transport if macro roughness is not taken into account. The simulated bedload transport is up to 10 times higher than the reconstructed transport. The comparison to the reconstructed bedload transport indicates that macro roughness resistance is probably non-negligible in modelling steep headwater streams. Literature confirms the importance of taking into account increased flow resistance due to macro roughness to obtain better agreement with observed and calculated bedload transport rates, e.g. Palt (2001), Rickenmann (2001, 2005), Rickenmann and Koschni (2010), Yager et al. (2007), Chiari and Rickenmann (2011). This can be explained by considering that the transport capacity formulas were derived from laboratory flume experiments with more or less uniform bed materials. Therefore, they do not include effects of increased flow resistance due to irregular bed form structures and shallow flows. The associated energy losses can be considered in the simulations and the parameter α is sensitive, requiring a value of around 1.5 in order to provide an acceptable fit between the reconstructed and the simulated sediment transport. Discharge based macro roughness resistance corrections turned out to be better suited for the estimation of energy losses in the rectangular cross-sections of TOPKAPI (setup M3). This is consistent with the fact that the finer river bed discretization of SETRAC enables a better simulation of the water levels whereas in TOPKAPI the water volume is equally distributed over the entire cross-section.

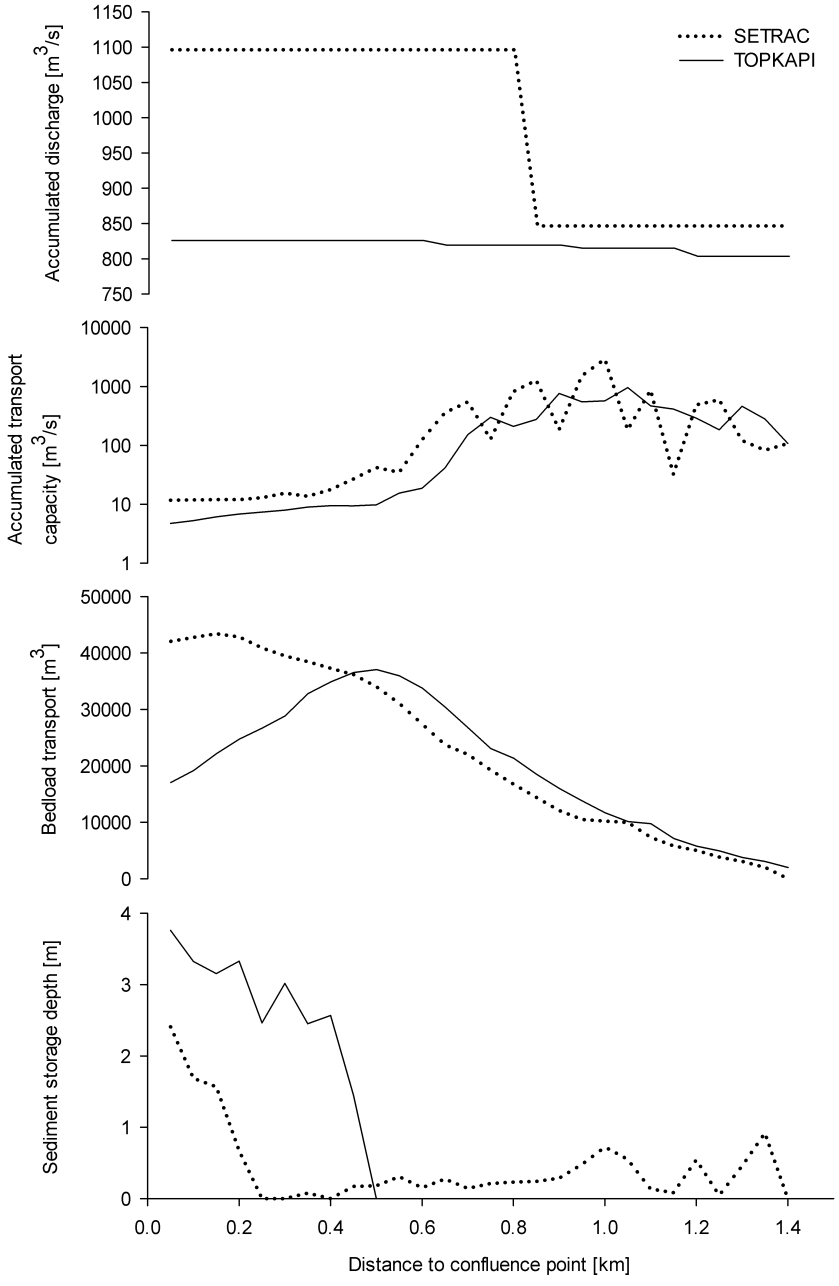

Fig. 7. Comparison of SETRAC and TOPKAPI for the tributary Spigge. **A**: Accumulated discharge over the simulation period for each cross-section element, **B**: accumulated transport capacity, **C**: bedload transport of each cross-section of the entire simulation period, **D**: sediment storage depth of the last time step.

The comparison of the two models additionally revealed that differences can be observed at the confluence point of Spigge and Chiene. This is due to the spatial discretizations of the rivers on grid cell level and to differences in sediment transport simulations of the Spigge. In TOPKAPI the confluence point of Spigge and Chiene and the lower cross-sections of Spigge are all covered by one grid cell which already holds the discharge contributions of the Spigge although on the sub-grid level the two rivers are still separated. The geometric correction introduced in TOPKAPI by shifting the Spigge sub-grid cross-sections by one grid cell, allows for a better representation of the hydraulic conditions, but cannot compensate for the finer representation of SETRAC. Therefore, the flow conditions are different between the two spatial discretizations of SETRAC and TOPKAPI. Furthermore, the hydraulic simulations of the Spigge itself differ due to the predefined locations of the input hydrographs of SETRAC. Figure 7a shows a significant jump of the accumulated water

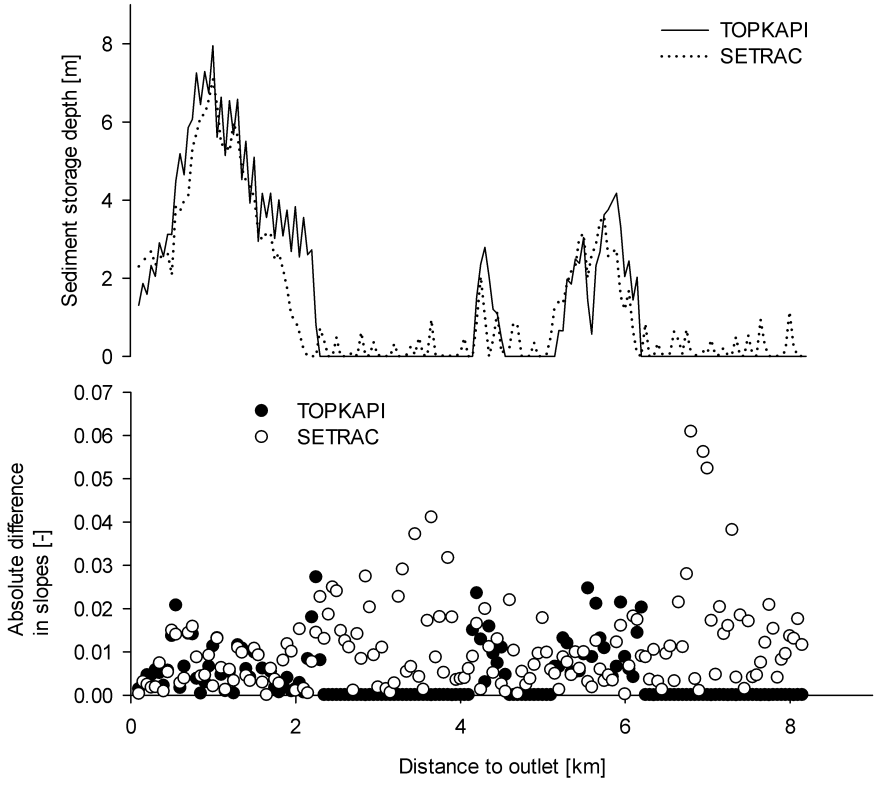

Fig. 8. Comparison of sediment storage depths and slope developments of SETRAC and TOPKAPI. **A**: Simulated sediment storage depths by TOPKAPI and SETRAC for the last simulation time step; **B**: absolute differences between the bed rock slope and the slopes provided by TOPKAPI and SETRAC for the last simulation time step.

discharge at 0.8 km which is caused by a newly assigned hydrograph at this cross-section (SETRAC is limited by the number of hydrographs that can be assigned to a simulation system). TOPKAPI simulates more stable but lower potential transport rates, whereas SETRAC provides values almost three times higher than TOPKAPI (e.g. at 1.0 km in Fig. 7b). This causes an increased deposition simulated by TOPKAPI between the confluence point and 0.5 km (Fig. 7d). The simulated sediment transport at the confluence point of Spigge and Chiene is more than double in SETRAC (Fig. 7c). Therefore, less sediment is provided to the river Chiene in the TOPKAPI simulation, which is one reason for the lower sediment transport rates at the cross-sections downstream of the confluence point. However, the different sediment fluxes of the Spigge cannot explain the entire difference between the two models. Simulation results of TOPKAPI with the sediment fluxes taken from SETRAC as input to the Chiene river at the confluence point provide an improvement (not shown here) and the peak becomes more visible but TOPKAPI still delivers bedload transport rates lower than SETRAC.

The fluctuations in SETRAC's bed slope calculations are more pronounced at locations prone to bed erosion. TOPKAPI simulates empty storages between 2.5 and 4.2 km and from 6.2 km upstream (Fig. 8a), whereas SETRAC still has fluctuating sediment storage depths between 0 and around 1 m, which can be explained by the wedge shaped erosion and deposition volumes calculated in SETRAC (see Chiari, 2008 for details). The slope of TOPKAPI is equal to the bed rock slope in these areas as expressed in absolute differences between TOPKAPI, SETRAC and bed rock slopes in Fig. 8b. The most pronounced differences of SETRAC's slopes can be observed at the high erosion areas due to the fluctuating storage levels. The temporal development of the slope in SETRAC shows slope patterns similar for the first and the last time step for reaches where the bed sediment is eroded. In depositional reaches the slope becomes more homogeneous, whereas in erosion reaches the channel gradient is shifted one cross-section downstream if the sediment storage is (nearly) emptied. The main difference between SETRAC and TOPKAPI is the wedge shaped sediment redistribution approach of SETRAC. TOPKAPI with its area-based erosion and deposition simulations (sediment volumes are shifted from one cell to the other without further modifications as conversely done in SETRAC) delivers less fluctuations in erosion reaches but fluctuations can still be observed in depositional reaches between 1 and 2.5 km in Fig. 8a.

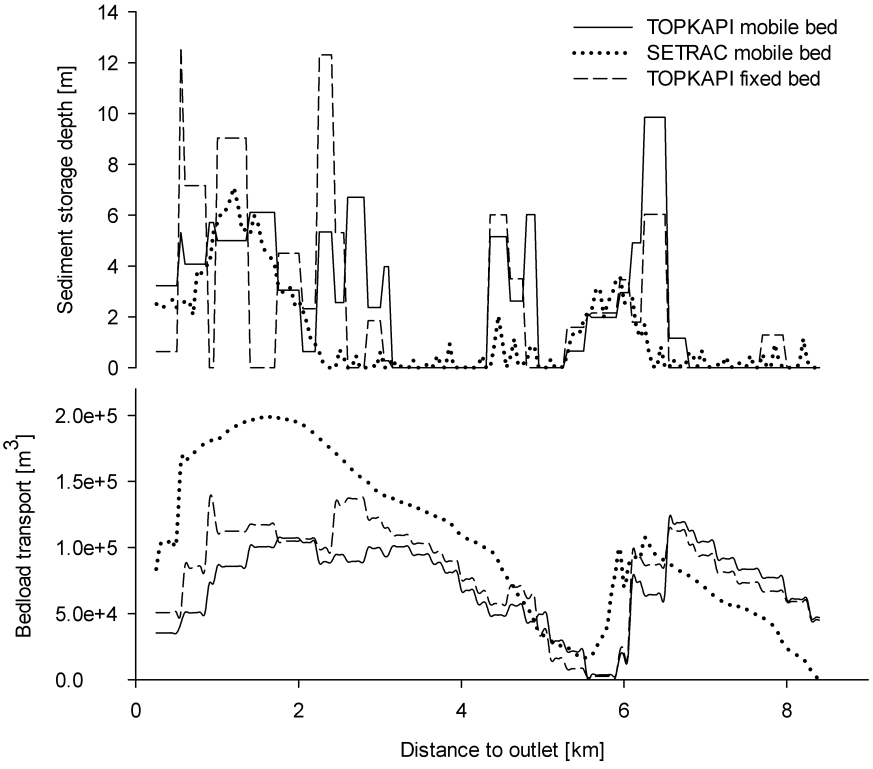

Fig. 9. Comparison of sediment transport simulations of TOPKAPI on the grid level with SETRAC. **A**: Simulated sediment storage depths (with mobile and fixed beds); **B**: bedload transport without correction for high flow resistance.

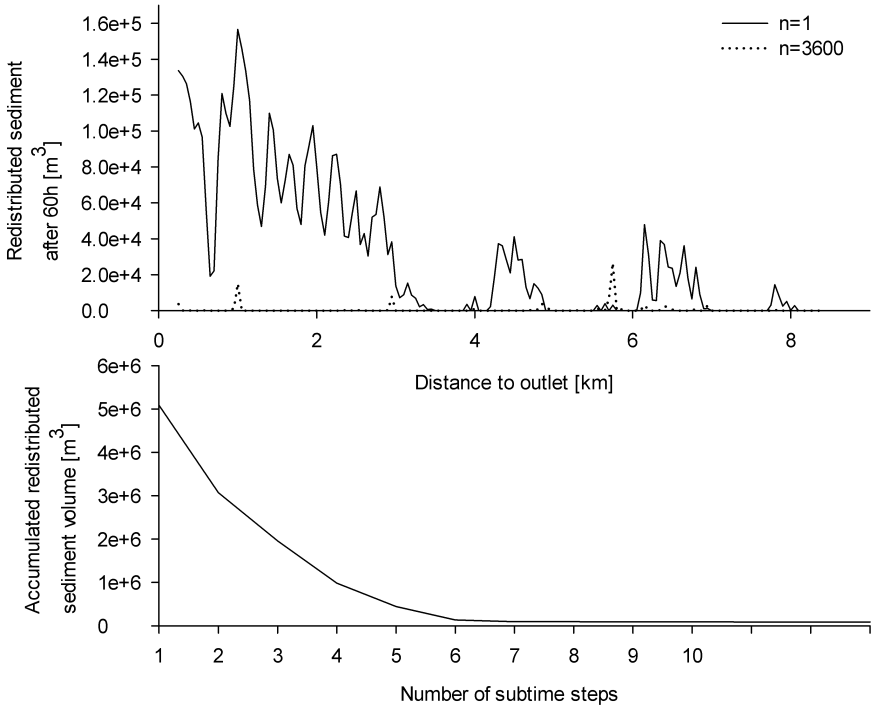

Fig. 10. Effect of sub-time step modelling. **A**: Artificially redistributed sediment along the channel; **B**: accumulated, redistributed sediment volumes simulated with different temporal resolutions.

Table 2. Advantages and disadvantages of TOPKAPI and SETRAC.

	TOPKAPI	**SETRAC**
Advantages	CPU time	Detailed representation of channel cross-sections
	Direct coupling of hydrological and channel processes	Graphical user interface with many visualization possibilities and geo-referenced representation of the channel network
	Simulations at different spatial scales	Internal discretization selectable by the user for sensitivity analysis
		No selection of calculation time step required (model decides on the maximum allowed time step for stable calculation)
		One grain model and fractional bedload transport calculations
		Results can be stored as preformatted A0 DXF files for practical applications and as text files for detailed analysis
Disadvantages	Only rectangular channel geometry	CPU time
	Artificial redistribution in order to avoid blocked channels	External simulations of the hydrology required
	Limited to steep mountain rivers due to kinematic wave approximation	
	No counter slopes or backwater effects considered	
	Limited to bedload transport (no suspended load or washload)	

The efficiency of the sub-grid modelling technique in TOPKAPI becomes obvious if simulation results of sediment transport using the general grid level are compared to SETRAC (Fig. 9). To demonstrate this simulations with the M1 setup have been performed with the sub-grid procedure switched on and off, to mimic respectively a mobile (solid line in Fig. 9) and fixed (dashed line in Fig. 9) river bed. The geometrical information (width, initial slope and initial storage level) have been taken from the cross-sections which are covered by the respective grid cells as mean values. Also in the case with inactive sub-grid the basic pattern of the SETRAC bedload transport simulations is reproduced (Fig. 9b), however lower transport rates are simulated. Interestingly, the model run with a fixed bed slope provides sediment transport rates closer to SETRAC than the one with variable bed slope especially between 0 and 5 km. However, the storage heights do not agree well with the SETRAC results (Fig. 9a). This shows that for a first assessment sediment transport simulations using the grid level can already provide estimates of acceptable reliability, especially considering the significantly low required amount of geometrical information. However, the overall comparison shows that the sub-grid modelling scheme significantly improves the simulation results, especially when sediment storage depths (Figs. 6 and 8a) and the slope evolution (Fig. 6) are considered.

It is finally interesting to discuss the effect of the sub-time step modelling, which is shown in Fig. 10. In order to avoid the blocking of the channel the model operates a redistribution of the sediment (see Sect. 2.3.2 above for details). The relative number of redistributions in Fig. 10a, i.e. the total number of artificial redistributions divided by the total number of time steps (number of sub-time steps $\times$ number of global time steps), shows that the artificial redistribution of additional sediment volumes significantly reduces with increasing number of sub-time steps. With smaller time steps (e.g. 1 s), the transported sediment volume per time step is smaller than with larger time steps (e.g. 1 h), thus the chance of blocking the channel is smaller when using the mobile bed approach, which adjusts the slopes at the end of each time step. Interestingly, the redistributed sediment volumes in Fig. 10b already converge at a relatively small number of sub-time steps, n, and $n = 7$ (equivalent to a time step of 514.3 s) provides a total redistribution volumes comparable to that obtained for $n = 3600$ (equivalent to a time step of 1 s). Thus the artificial redistribution can be minimized by a sufficiently small sub-time step.

8 Conclusions and outlook

In this study we developed further the distributed hydrological model TOPKAPI and implemented a bedload sediment transport module. The model has been tested against the more sophisticated SETRAC model. The newly implemented sediment transport module in the distributed in space

and continuous in time hydrological model TOPKAPI enables the simulation of sediment transport rates, erosion and deposition patterns and bed slope developments in a river channel network. This implementation offers new and interesting perspectives to model erosion and sediment transport across an entire catchment, not only throughout one storm rainfall event, but also over longer terms, with results that are comparable to specialised models based on computationally demanding hydraulic schemes. Thus, since the transport module is directly coupled to the hydrological model, effects of changes in the hydrological cycle on the sediment transport patterns can be studied.

The performance of the sediment transport accounting TOPKAPI compared to a more sophisticated, specialised sediment transport model (SETRAC) is satisfying. The advantages and disadvantages of the two models are summarized in Table 2. The major innovation of this study is the implementation of the sub-grid modelling scheme, which significantly improves the simulation of the bedload sediment transport compared to the coarser grid level simulation. The assumption that discharge can be simulated at the grid level and used for all sub-grid sections within that grid cell provides reliable sediment discharge simulations. This approach exhibit inaccuracies at confluence points, for which a more sophisticated solution for flow partitioning should be used based on the ratio of inflowing discharge from the upstream cells.

At the present stage of development TOPKAPI does not consider yet a feedback mechanism of the mobile bed on the hydraulic simulations. This limitation can be reasonable if the slope changes are moderate during an event. However, an up-scaling of the sub-grid geometry to account at the model general grid level for changes induced by erosion and sediment transport should be investigated further. Moreover, we have shown that sediment transport simulations in the modified TOPKAPI are computationally quite efficient, since the model requires only 40 s on a standard desktop computer for the simulation of the 60 h event with 3600 internal sub-time steps, especially when compared to an equally performing specialised model requiring a thousand times longer simulation.

Finally, while we recognise that the model requires to be further validated on additional real events, we believe that the study shows a direction in which integrated models, which combine the modelling of catchment hydrological response and of processes driven by it, can evolve. Recent floods in several mountain regions of Switzerland and Europe have shown that there is indeed an impelling need, both for design purposes and in real-time, of models that can efficiently simulate across different catchment scales the multiple effects of storm rainfall, such as the serial dependence of soil slips, diffused erosion and channel sediment transport. The sediment accounting TOPKAPI model, which has been presented in this study, aims at tracing a path that can cover that need.

Acknowledgements. We highly acknowledge the inputs and discussions of Francesca Pellicciotti. This study has been carried out within the project APUNCH (Advanced Process UNderstanding and prediction of hydrological extremes and Complex Hazards) funded by the Competence Center Environment and Sustainability (CCES) of the ETH Domain (Switzerland).

Edited by: J. Freer

References

Bahadori, F., Ardeshir, A., and Tahershamsi, A.: Prediction of alluvial river bed variation by SDAR model, J. Hydraulic Res., 44(5), 614–623, 2006.

Badoux, A. and Rickenmann, D.: Berechnung zum Geschiebetransport während der Hochwasser 1993 und 2000 im Wallis, Wasser Energie Luft, 3, 217–226, 100. Jahrgang, 2008 (in German).

Bathurst, J. C., Li, R.-M., and Simons, D. B.: Resistance equation for large-scale roughness, J. Hydr. Div., 107, 1593–1613, 1981.

Beffa, C.: 2D-Simulation der Sohlenreaktion in einer Flussverzweigung, Österreichische Wasser- und Abfallwirtschaft, 42(1–2), 1–6, 2005 (in German).

Chiari, M.: Numerical modelling of bedload transport in torrents and mountain streams. PhD dissertation, University of Natural Resources and Applied Life Sciences, Vienna, Austria, 2008.

Chiari, M. and Rickenmann, D.: Back-calculation of bedload transport in steep channels with a numerical model, Earth Surf. Process. Landforms, 36, 805–815, doi:10.1002/esp.2108, 2011.

Chiari, M., Scheidl, C., and Rickenmann, D.: Assessing morphologic changes caused by torrential flood events with airborne lidar data, in: Global Change – Challenges For Soil Management, Adv. Geoecol., 41, 192–202, Catena Verlag, ISBN: 978-3-923381-57-9, 2010a.

Chiari, M., Friedl, K., and Rickenmann, D.: A one dimensional bedload transport model for steep slopes, J. Hydraul. Res., 48(2) 152–160 doi:10.1080/00221681003704087, 2010b.

Corripio, J. G.: Vectorial algebra algorithms for calculating terrain parameters from DEMs and solar radiation modelling in mountainous terrain, Int. J. Geogr. Inf. Sci., 17(1), 1–23, 2003.

Deyhle, C., Glugla, G., Golf, W., v. Hoyningen Huene, J., Kalweit, H., Olbrisch, H., Richter, D., Wendling, U., Wessolek, G., and Wittenberg, H.: Ermittlung der Verdunstung von Land- und Wasserflächen. Technical Report 238, Deutscher Verband für Wasserwirtschaft und Kulturbau e.V. (DVWK), 1996.

Doten, C. O., Bowling, L. C., Lanini, J. S., Maurer, E. P., and Lettenmaier, D.,P.: A spatially distributed model for the dynamic prediction of sediment erosion and transport in mountainous forested watersheds, Water Resour. Res. 42, W04417, doi:10.1029/2004WR003829, 2006.

Fehr, R.: A method for sampling very coarse sediments in order to reduce scale effects in movable bed models. Proc. Symp. Scale effects in modelling sediment transport phenomena, Toronto, IAHR, Delft, 383–397, 1986.

Hassan, M. A., Church, M., and Lisle, T. E.: Sediment transport and channel morphology of small, forested streams, J. Am. Water Resour. Assoc. 41(4), 853–876, 2005.

Hock, R. and Noetzli, C.: Areal melt and discharge modelling of Storglaciaren, Sweden, Ann. Glaciol., 24, 211–216, ISSN: 0260-3055, ISBN: 0-946417-19-9, 1997.

Khorram, S. and Ergil, M.: Most Influential Parameters for the Bed-Load Sediment Flux Equations Used in Alluvial Rivers, J. Am. Water Resour. As., 46(6), 1065–1090, 2010.

Liu, Z. and Todini, E.: Towards a comprehensive physically-based rainfall-runoff model, Hydrol. Earth Syst. Sci., 6, 859–881, doi:10.5194/hess-6-859-2002, 2002.

Liu, Z., Martina, M. L. V., and Todini, E.: Flood forecasting using a fully distributed model: application of the TOPKAPI model to the Upper Xixian Catchment, Hydrol. Earth Syst. Sci., 9, 347–364, doi:10.5194/hess-9-347-2005, 2005.

Lokale lösungsorientierte Ereignisanalyse (LLE) Reichenbach. In Technischer Bericht. Emch + Berger AG, Spiez; Hunziker, Zarn & Partner AG, Aarau; Geotest AG, Zollikofen. Tiefbauamt Kanton Bern, Bern, unpublished, 2006 (in German).

Mathys, N., Brochot, S., Meunier, M., and Richard, D.: Erosion quantification in the small marly experimental catchments of Draix (Alpes de Haute Provence, France): Calibration of the ETC rainfall-runoff-erosion model, Catena, 50, 527–548, 2003.

MeteoSchweiz: Starkniederschlagsereignis August 2005. Arbeitsberichte der MeteoSchweiz 211, Bundesamt für Meteorologie und Klimatologie, 63 pp., 2006.

Meyer-Peter, E. and Mueller, R.: Formulas for bedload transport, 2nd IAHR Congress,. Stockholm, Appendix 2, 39–64, 1948.

Nitsche, M., Rickenmann, D., Turowski, J., Badoux, A., and Kirchner, J.: Evaluation of bedload transport predictions using flow resistance equations to account for macro-roughness in steep mountain streams, Water Resour. Res., 47, W08513, doi:10.1029/2011WR010645, 2011.

Palt, S.: Sedimenttransporte im Himalaya-Karakorum und ihre Bedeutung für Wasserkraftanlagen, Mitteilung 209, Institut für Wasserwirtschaft und Kulturtechnik, Universität Karlsruhe, Karlsruhe Germany, 2001 (in German).

Papanicolaou, A., Bdour, A., and Wicklein, E.: One-dimensional hydrodynamic/sediment transport model applicable to steep mountain streams, J. Hydraulic Res., 42(4), 357–375, 2004.

Pellicciotti, F., Brock, B., Strasser, U., Burlando, P., Funk, M., and Corripio, J.: An enhanced temperature-index glacier melt model including the shortwave radiation balance: development and testing for Haut Glacier d'Arolla, Switzerland, J. Glaciol., 51(175), 573–587, 2005.

Recking, A., Frey, P., Paquier, A., Belleudy, P., and Champagne, J. Y.: Feedback between bed load transport and flow resist-ance in gravel and cobble bed rivers, Water Resour. Res., 44, W05412, doi:10.1029/2007WR006219, 2008.

Reichel, G., Fäh, R., and Baumhackl, G.: FLORIS-2000: Ansätze zur 1.5D Simulation des Sedimenttransportes im Rahmen der mathematischen Modellierung von Fließvorgängen, in: Internat, Symposion "Betrieb und Überwachung wasserbaulicher Anlagen", 2000 (in German).

Rickenmann, D.: Bedload transport capacity of slurry flows at steep slopes. Mitteilung, 103, Versuchsanstalt für Wasserbau, Hydrologie Glaziologie, ETH Zurich, Zurich, 1990.

Rickenmann, D.: Hyper-concentrated flow and sediment transport at steep slopes, J. Hydraul. Eng., 117(11), 1419–1439, 1991.

Rickenmann, D.: An alternative equation for the mean velocity in gravel-bed rivers and mountain torrents, Proc. Nat. Conf. Hydraulic Engineering, Buffalo NY 1, 672–676, editd by: Cotroneo, G. V. and Rumer, R. R., ASCE, New York, 1994.

Rickenmann, D.: Fliessgeschwindigkeit in Wildbächen und Gebirgsflüssen, Wasser, Energie, Luft., 88(11/12), 298–304, 1996 (in German).

Rickenmann, D.: Comparison of bed load transport in torrents and gravel bed streams, Water Resour. Res. 37(12), 3295–3305, 2001.

Rickenmann, D.: Geschiebetransport bei steilen Gefällen. Mitteilung 190, 107–119. Versuchsanstalt fü r Wasserbau, Hydrologie und Glaziologie, ETH Zurich, Zurich, 2005 (in German).

Rickenmann, D., Chiari, M., and Friedl, K.: SETRAC – A sediment routing model for steep torrent channels. River Flow 2006 1, 843–852, edited by: Ferreira, R., Leal, E. A. J., adn Cardoso, A., Taylor & Francis, London, 2006.

Rickenmann, D. and Koschni, A.: Sediment loads due to fluvial transport debris flows during the 2005 flood events in Switzerland, Hydrol. Process, 24, 993–1007, 2010.

Rinderer, M., Jenewein, S., Senfter S., Rickenmann, D., Schöberl, F., Stötter, J., and Hegg, C.:. Runoff and bedload transport modelling for flood hazard assessment in small alpine catchments - the PROMAB-GIS model, in: Sustainable Natural Hazard Management in Alpine Environments, edited by: Veulliet, E., Stötter, J., and Weck-Hannemann, H.. Springer, Heidelberg, New York, 69–101, 2009

Scheidl, C., Rickenmann, D., and Chiari, M.: The use of airborne LiDAR data for the analysis of debris flow events in Switzerland, Nat. Hazards Earth Syst. Sci., 8, 1113–1127, doi:10.5194/nhess-8-1113-2008, 2008.

Todini, E. and Ciarapica, L.: The TOPKAPI model, in: Mathematical models of large watershed hydrology, edited by: Singh, V. P., Water Resources Publications, Littleton, Colorado, USA, 2001.

Todini, E. and Mazzetti, C.: TOPKAPI User manual and references, PROGEA, 2008.

Wicks, J. M. and Bathurst, J. C.: SHESED:Aphysically based, distributed erosion and sediment yield component for the SHE hydrological modelling system, J. Hydrol., 175, 213–238, 1996.

Yager, E. M., Kirchner, J. W., and Dietrich, W. E.: Calculating bed load transport in steep boulder bed channels, Water Resour. Res., 43(7), W07418, doi:10.1029/2006WR005432, 2007.